Composites Part B 183 (2020) 107657

Contents lists available at ScienceDirect

Composites Part B

journal homepage: www.elsevier.com/locate/compositesb

Stress analysis of urban gas pipeline repaired by inserted hose lining method

Hongfang Lu [a,b], Xiaonan Wu [c,*], Houming Ni [d], Mohammadamin Azimi [b], Xuanchen Yan [e], Yingqi Niu [a]

[a] State Key Laboratory of Oil and Gas Reservoir Geology and Exploitation, Southwest Petroleum University, Chengdu, 610500, China
[b] Trenchless Technology Center, Louisiana Tech University, Ruston, LA, 71270, United States
[c] School of Civil Engineering and Architecture, Southwest Petroleum University, Chengdu, 610500, China
[d] Asoe Hose Manufacturing Inc., Taizhou, 225319, China
[e] QuakeWrap, Inc., Tucson, AZ, 85756, United States

ARTICLE INFO

Keywords:
Trenchless technology
Inserted hose lining
Urban gas pipeline
Stress analysis
Finite element analysis (FEA)

ABSTRACT

Inserted hose lining (IHL) is a trenchless technology with high application potential in repairing urban gas pipelines. Since the application of this technology in gas pipelines is still in the developing stage, it is necessary to study its feasibility. Based on the mechanical properties of the composite lining material used in this technology, the stress analysis is carried out using ANSYS Workbench software. In this paper, two kinds of aging pipelines with defects are considered, and the repair effect of IHL technology is studied. One is the pipeline with uniform corrosion defect, and the other is the pipeline with corrosion perforation defect. For the pipeline with uniform corrosion defect, the influences of residual thickness, diameter, pressure, and buried depth on pipeline stress are studied. For the pipeline with corrosion perforation defect, the influences of the corrosion perforation position, the corrosion perforation size, diameter, and pressure on pipeline stress are studied. According to the allowable stress of the steel pipeline, the applicable scope of the lining under different conditions is obtained. Based on the analysis results, the main conclusions are as follows: (1) IHL method can effectively reduce the stress of the old pipeline, and the old pipeline is the primary pressure bearing component. (2) Under uniform corrosion conditions, the residual thickness is inversely related to the pipe stress, the pressure and diameter are positively correlated with the pipe stress. (3) Under the condition of corrosion perforation, it is the most dangerous situation that the corrosion hole is near the pipe bottom.

1. Introduction

The pipeline is the most effective way to transport natural gas, which is of great significance for the allocation of energy [1]. As time goes on, many pipelines enter the aging stage, and it is difficult to avoid problems such as corrosion and leakage. Therefore, pipeline repair has a vast market currently and in the future. It is estimated that the global oil and gas pipeline repair market value will reach 10 billion US dollars by 2019 [2]. In the context of promoting green construction [3,4], trenchless technology is undoubtedly the primary option for pipeline repair.

Trenchless technology refers to the technique of installing, renewing (repairing or replacing), and inspecting pipelines by directional drilling or other means without excavation or minimal excavation of the surface. The technology has little impact on the surface traffic and has the characteristics of less carbon footprint, less noise, faster speed, and less investment [5]. Among the trenchless repair methods, the technologies that are more suitable for gas pipelines mainly include cured-in-place pipe (CIPP), sliplining (SL), deformed and reformed (DR), fold and form (FF), and spray-in-place pipe (SIPP) and inserted hose lining (IHL) [2,6].

Among these trenchless repair technologies, CIPP is currently the most popular method, which appeared in the 1970s and was invented by British engineer Eric Wood [7]. The method immerses the epoxy resin or the unsaturated resin on the impervious hose and uses water or air as a power to adhere to the inner wall of the old pipe, and then cured by ultraviolet or steam to form a new lining in the pipe. The technology was introduced into the United States in 1977, and then spread to many countries and has continuously been improved. SL is an early and

* Corresponding author.
E-mail address: wuxiaonanswpu@126.com (X. Wu).

https://doi.org/10.1016/j.compositesb.2019.107657
Received 1 April 2019; Received in revised form 22 October 2019; Accepted 28 November 2019
Available online 6 December 2019

Table 1
Advantages and limitations of various trenchless repair methods [2].

Technology	Merit	Limitation
CIPP	The process is simple, the construction speed is fast, the pipeline transportation capacity is improved, and the economy is good.	High requirements for construction equipment and high professional requirements for operators.
SL	The construction process is simple, the construction speed is fast, the economy is good, professional equipment is not needed, and the skill requirements of the operator are low.	It is necessary to grout in the annulus, the section loss is substantial, but the transport capacity may not be reduced.
DR	The construction speed is fast, the section loss is small, and structural repair and non-structural repair can be performed.	The construction equipment is expensive, and the construction cost is high. Construction is greatly affected by the state of the old pipeline.
FF	The space required for construction is small, the cleaning requirements for the old pipeline are low, the construction speed is fast, and the construction process is simple.	Structural damage may occur in the construction process, and the construction is greatly affected by the status of the old pipeline.
SIPP	It can prolong the service life of the pipeline, effectively alleviate the corrosion, reduce the maintenance cost.	Old pipes need to have certain structural integrity.
IHL	The transport capacity will not be affected. It can greatly improve corrosion resistance.	Cannot pass a large angle bend.

economical trenchless repair method that drags a new pipe directly into the old pipe. Due to the gap between the two pipes, it is usually necessary to grout in the annulus to form a "pipe-in-pipe" structure [8]. Besides, there are other methods in the trenchless market, such as SIPP and DR. Various methods have their advantages and limitations, as shown in Table 1.

Concerning the stress analysis of the lining, Wang and Yang [9]used ANSYS software to analyze the residual thermal stress of ceramic lined composite pipe. They obtained that reasonable adjustment of the thickness of high-temperature synthesis layer can improve the service life of the composite pipe. Li et al. [10] studied the analytical solution of elastic buckling of CIPP lining under external hydrostatic pressure. Rueda et al. [11] found that after the polymer lining pipeline repaired the oil pipeline, when the inner pressure was high, the carbon dioxide and methane in the oil would penetrate the space between the inner pipe and outer pipe. When the pressure of the pipe was reduced, the gas would bring the external pressure to the lining pipe, and it would lead to the buckling failure of the lining pipeline in some cases. Chuk et al. [12] analyzed the stress of pipe repaired by the CIPP method and discussed the effects of different liners on reducing pipe stress. Kim et al. [13] used the finite element method to analyze the buckling behavior of elastic lining on the cracked cylindrical shell and studied the influence of crack geometry, thickness, and other factors. The results show that the crack is mainly affected by crack orientation and lining thickness. Shou and Chen [14] used ABAQUS software to analyze the mechanical behavior of pipes repaired by the CIPP method, and the result shows that it can strengthen damaged pipes by reducing stress concentration.

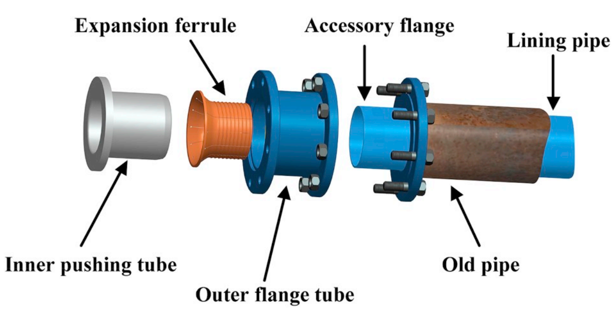

Fig. 1. Pipe and pipe fittings for the IHL method [15,16].

Fig. 3. Physical diagram of the lining.

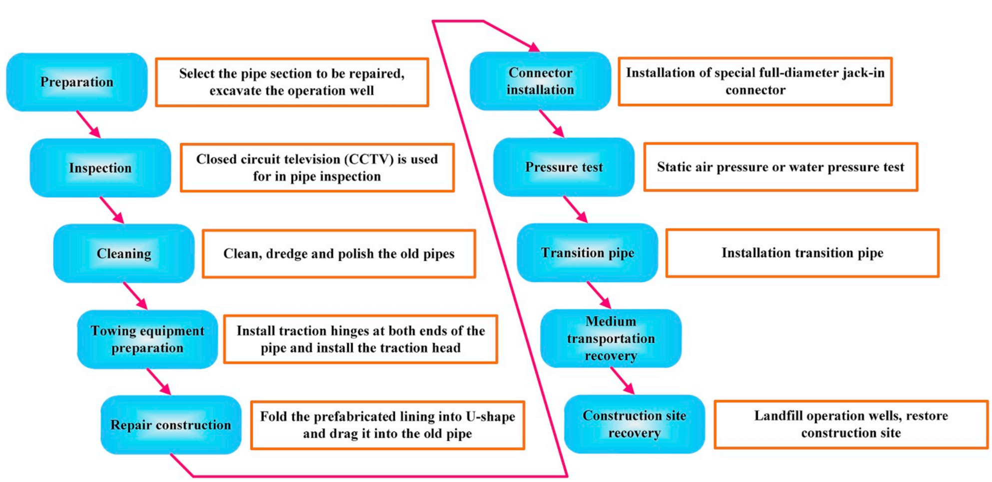

Fig. 2. The construction process of the IHL method [15,16].

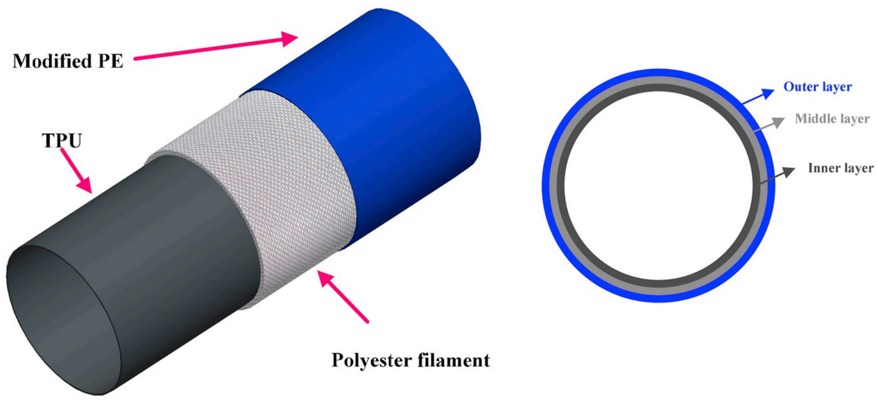

Fig. 4. The schematic diagram of the lining structure.

Table 2
The properties of the lining material [22].

Layer	Material	Property parameters	Value
Inner	TPU	Elastic modulus (GPa)	0.1
		Poisson's ratio	0.48
		Density (kg/m^3)	1200
		Thickness (mm)	2.0
Middle	Polyester filament	Elastic modulus (GPa)	15.0
		Poisson's ratio	0.35
		Density (kg/m^3)	1440
		Thickness (mm)	2.0
Outer	Modified PE	Elastic modulus (GPa)	1.07
		Poisson's ratio	0.41
		Density (kg/m^3)	960
		Thickness (mm)	2.0

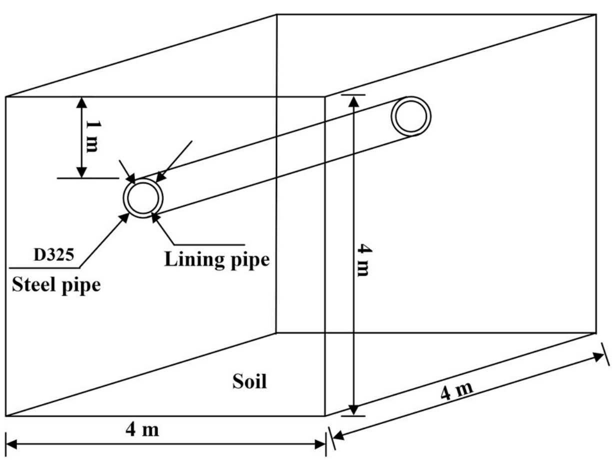

Fig. 5. Geometric model of the pipe-soil system.

The IHL method is an essential component of the trenchless repair method. It was initially applied to water pipelines and has been used in gas pipelines in recent years. As the technology is still in the development stage, it is necessary to perform stress analysis on the pipeline repaired by this method, thus providing a basis for construction and design. The rest of the paper is organized as follows: Section 2 provides a brief introduction to the IHL method. Section 3 introduces the theory of composite lining materials. Section 4 describes the research case and finite element analysis (FEA) process in this paper. Section 5 shows the results of the FEA. Section 6 analyzes the relevant influencing factors and stress sensitivity. Section 7 summarizes the main conclusions of this paper.

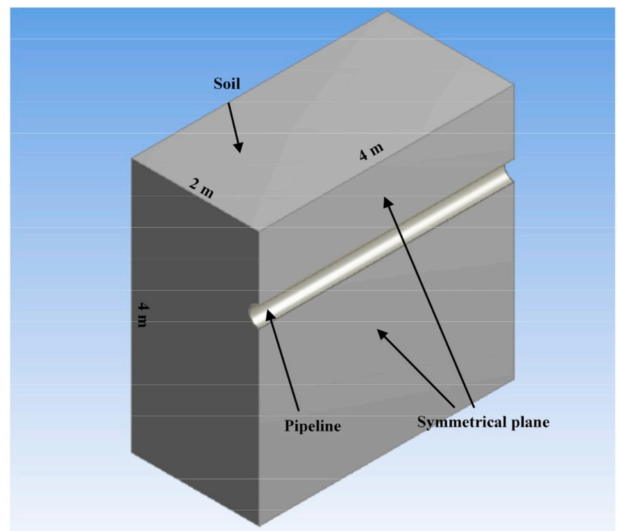

Fig. 6. Pipeline-soil system used in the simulation.

Table 3
Steel pipeline parameters.

Material	Parameters	Value
Steel pipeline (20 Steel)	Pipeline size (mm)	325 × 4.8 (diameter × thickness)
	Buried depth (m)	1
	Elastic modulus (GPa)	202
	Poisson's ratio	0.3
	Density (kg/m^3)	7800
	Minimum yield strength (MPa)	245
	Tensile strength (MPa)	390
	Allowable stress (MPa)	130

Table 4
The parameters of the soil.

Material	Properties parameters	Value
Soil	Elastic modulus (MPa)	60
	Poisson's ratio	0.32
	Density (kg/m^3)	1900
	Cohesion (kPa)	15
	Internal friction angle (°)	15
	Dilation angle(°)	0

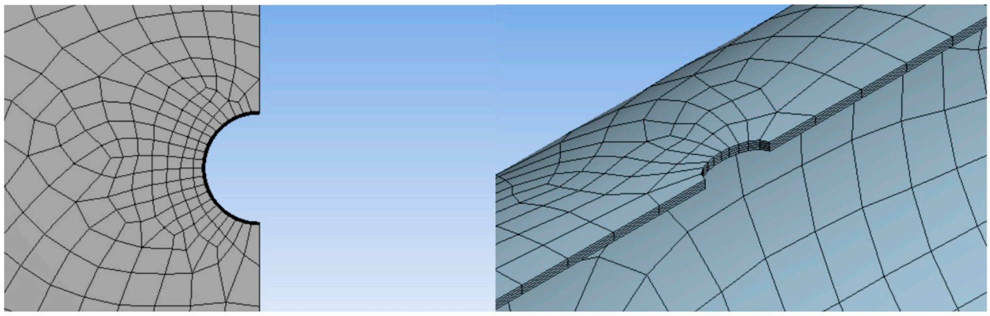

Fig. 7. The meshing of key locations. (a) Around the steel pipe; (b) Around the corrosion hole.

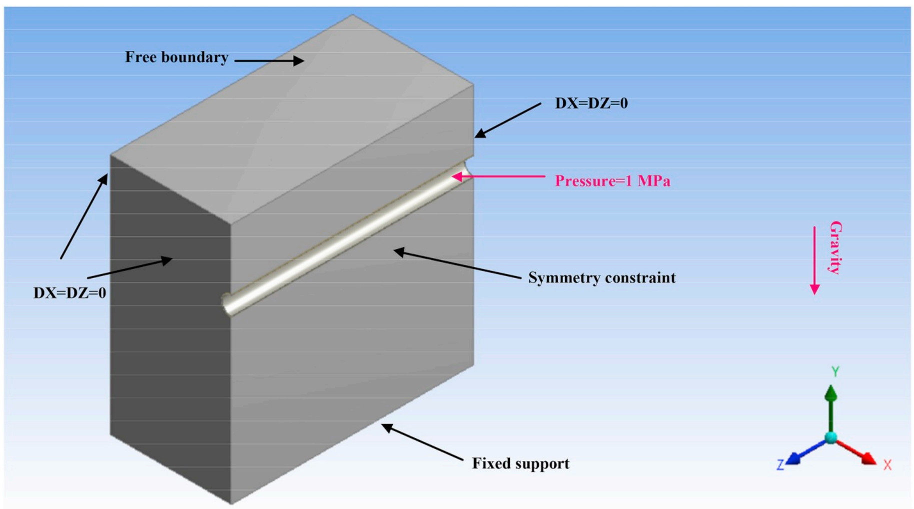

Fig. 8. Constraints and loads of the model.

2. Insert hose lining technology introduction

Insert hose lining (IHL) is a trenchless technology for repairing pressure pipes containing defects. It primarily consists of a soft reinforced hose lining material and connectors (see Fig. 1). Its basic construction process is first to fold the lining hose made in the factory into U-shape, pull it into the old pipe, and restore its cross-section to a circular shape by air, water, or steam. The IHL method is a non-structural repair method because there is no connection between the old pipe and the lining, making the lining work independently of the old pipe. Typically, special fittings are required at the end of the pipe to secure the lining. The lining is usually reinforced polyethylene and has a certain hardness so that it can be kept round in the old pipe even without internal pressure or with a small amount of external pressure. The IHL method has the characteristics of simple construction, can withstand high pressure, and can significantly extend the service life of the pipeline due to the corrosion resistance of the lining material. In addition, although the lining material has a certain thickness, and the cross-section of the pipe is reduced, the transport ability is not affected since the roughness of the inner surface of the material is small. Compared to CIPP, IHL technology is faster to construct and does not require curing equipment [15,16]. The specific construction process is shown in Fig. 2.

3. Composite properties

3.1. Interaction between materials

Compared with traditional materials, composite materials rely on different materials to bear and disperse loads. In the process of designing and using composite materials, it is necessary to consider the interaction and compatibility between different materials. The interface between matrix and reinforcement in the composite is essential because it can reflect the interaction between matrix and reinforcement. The interface between two component materials is not only a geometric intersection but also an interface layer with a certain thickness. Complex physical, chemical, and mechanical changes will be caused by the drastic changes in the chemical composition of the interface layer.

3.2. Basic mechanical properties of orthogonal fabric composites

A fabric made of mutually perpendicular warp and weft yarns is called an orthogonal fabric. In order to analyze the basic mechanical properties of the orthogonal fabric composite, it can be considered that the orthogonal fabric composite is composed of two layers of mutually perpendicular unidirectional fiber composite with the same matrix content, and its thickness is distributed according to the longitude and latitude of the fiber content [17]. The basic mechanical properties, i.e., elastic constant and basic strength, of the orthogonal matrix composite, can be calculated by the following equations [18,19]:

(1) Elastic modulus

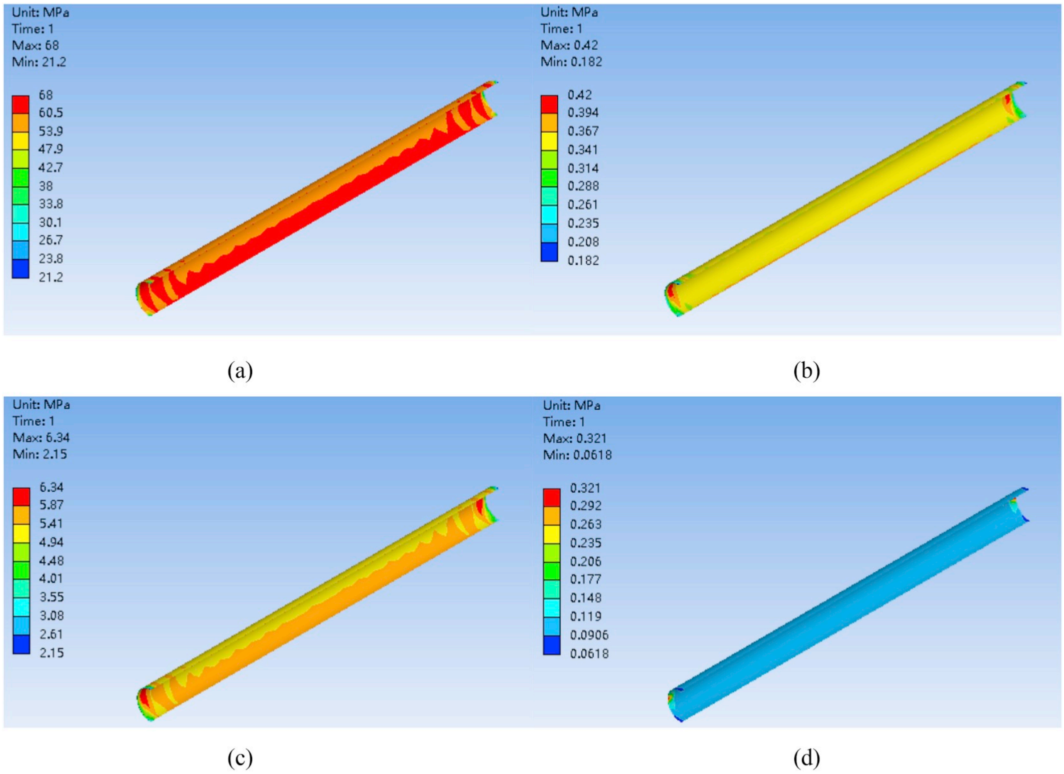

Fig. 9. The stress nephogram of the steel and lining. (a) Steel pipe; (b) Outer layer; (c) Middle layer; (d) Inner layer.

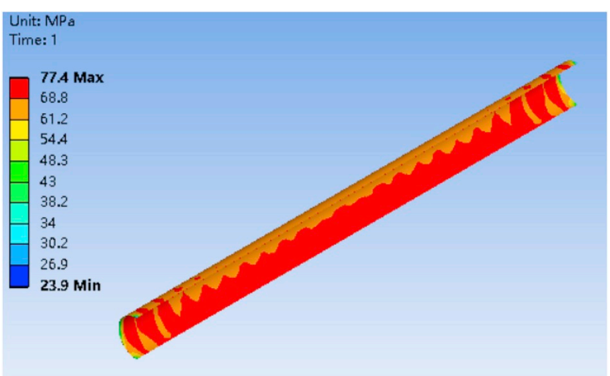

Fig. 10. The stress nephogram of the steel pipeline without lining.

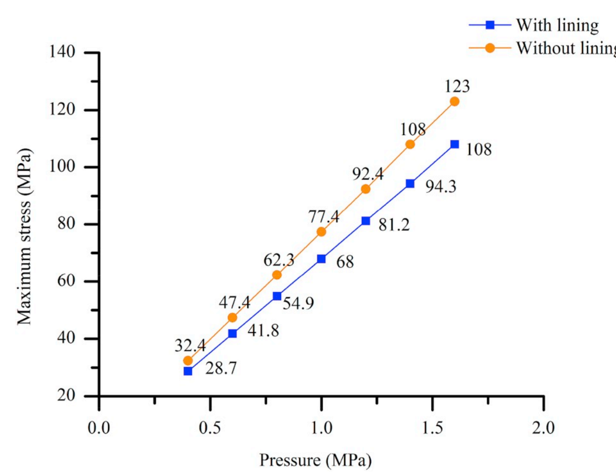

Fig. 11. Maximum stresses of steel pipes with and without lining under different pressures.

$$E_{wa} = K\left(E_1\frac{n_{wa}}{n_{wa}+n_{we}} + E_2\frac{n_{we}}{n_{wa}+n_{we}}\right), \tag{1}$$

$$E_{we} = K\left(E_1\frac{n_{we}}{n_{wa}+n_{we}} + E_2\frac{n_{wa}}{n_{wa}+n_{we}}\right) \tag{2}$$

where E_{wa} and E_{we} represent warp elastic modulus and weft elastic modulus of the orthogonal fabric composite, respectively; E_1 represents the longitudinal elastic modulus of unidirectional fiber composites; E_2 represents the transverse elastic modulus of unidirectional fiber composites; K is fabric ripple influence coefficient; n_{wa} represents the warp fiber content in the unit width; n_{we} represents the weft fiber content in the unit width.

(2) Poisson's ratio

$$\mu_{wa} = \mu_1 E_2\frac{n_{wa}+n_{we}}{n_{wa}E_2 + n_{we}E_1}, \tag{3}$$

$$\mu_{we} = \mu_L\frac{E_{we}}{E_{wa}}. \tag{4}$$

where μ_{wa} represents warp Poisson's ratio; μ_{we} represents weft Poisson's ratio; μ_L represents longitudinal Poisson's ratio.

(3) Shear elastic modulus

$$G = K\cdot G_{12}. \tag{5}$$

where G represents the shear elastic modulus of orthogonal fabric composites; G_{12} represents the in-plane shear modulus of unidirectional fiber composites.

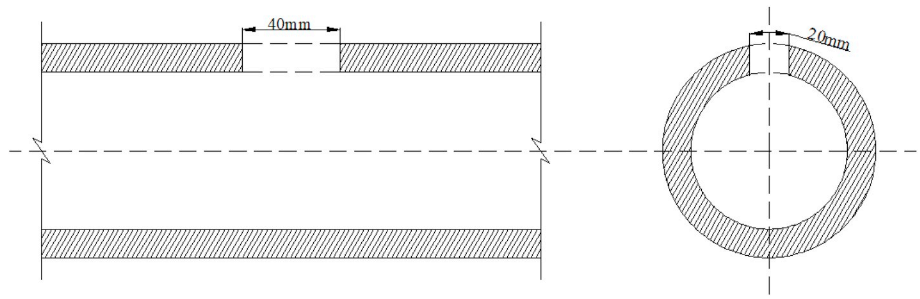

Fig. 12. Corrosion perforation geometric model.

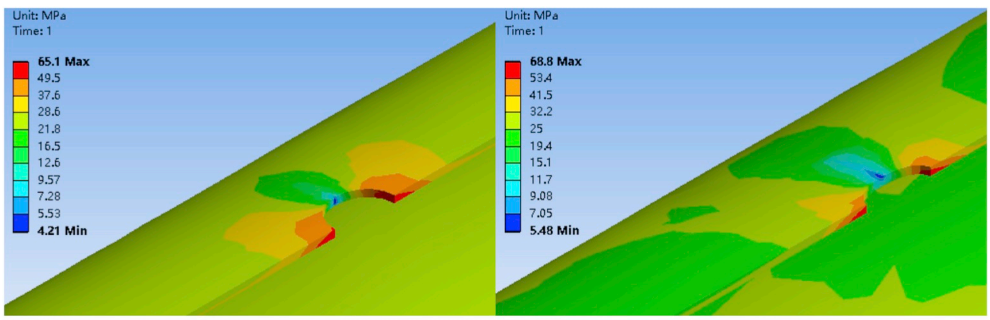

(a) (b)

Fig. 13. The stress nephogram of the steel pipeline with corrosion perforation after lining repair. (a) Circular corrosion hole condition; (b) Elliptical corrosion hole condition.

Table 5
The value ranges of the influencing factors.

Corrosion type	Influencing factor	Value range	Basic study conditions
Uniform corrosion	Residual thickness (mm)	2.0–4.0	Pressure = 1 MPa, buried depth = 1 m, nominal diameter = DN300
	Nominal diameter	DN100-DN600	Pressure = 1 MPa, buried depth = 1 m, residual thickness = 2 mm
	Pressure (MPa)	0.4–1.6	Buried depth = 1 m, nominal diameter = DN300, residual thickness = 2 mm
	Buried depth (m)	0.6–2.0	Pressure = 1 MPa, residual thickness = 2 mm, nominal diameter = DN300
Corrosion perforation	Corrosion perforation location	Top to bottom	Pressure = 1 MPa, pipeline size = DN300, buried depth = 1 m, perforation size (Long axis = 40 mm, short axis = 20 mm)
	Corrosion perforation diameter (mm)	20–90	Pressure = 1 MPa, pipeline size = DN300, buried depth = 1 m
	Pipe diameter	DN100-DN600	Pressure = 1 MPa, buried depth = 1 m, perforation shape = ellipse (Long axis = 40 mm, short axis = 20 mm)
	Pressure	0.4–1.6	Pressure = 1 MPa, buried depth = 1 m, pipeline thickness = 5 mm, perforation shape = ellipse (Long axis = 40 mm, short axis = 20 mm)

(4) Basic strength

$$X_{waT} = X_f \upsilon_f \frac{n_{wa}}{n_{wa} + n_{weL}} + X_m \left(1 - \upsilon_f \frac{n_{wa}}{n_{wa} + n_{weL}}\right), \tag{6}$$

$$X_{weT} = X_f \upsilon_f \frac{n_{we}}{n_{wa} + n_{we}} + X_m \left(1 - \upsilon_f \frac{n_{we}}{n_{wa} + n_{we}}\right), \tag{7}$$

$$X_{waC} = \varepsilon_{cr} E_f \upsilon_f \frac{n_{wa}}{n_{wa} + n_{we}} + \sigma_{mcr} \left(1 - \upsilon_f \frac{n_{wa}}{n_{wa} + n_{we}}\right), \tag{8}$$

$$X_{weC} = \varepsilon_{cr} E_f \upsilon_f \frac{n_{we}}{n_{wa} + n_{we}} + \sigma_{mcr} \left(1 - \upsilon_f \frac{n_{we}}{n_{wa} + n_{we}}\right). \tag{9}$$

where X_{waT} represents the warp tensile strength; X_{weT} represents the weft tensile strength; X_{waC} represents the warp compression strength; X_{weT} represents the weft compression strength; ε_{cr} represents the critical strain of fiber compression instability failure; σ_{mcr} represents the matrix stress of fiber compression instability failure; X_f represents the longitudinal strength of fiber materials; X_m represents the longitudinal strength of matrix material; υ_f represents the fiber volume content; E_f represents the elastic modulus of fiber material.

3.3. Failure criteria of composite materials

The failure criterion of composite materials generally refers to the failure criteria of the auxiliary layer. Failure criteria are commonly used to judge whether the composite material fails, mainly include maximum stress failure criterion, maximum strain failure criterion, the Tsai-Wu tensor polynomial failure criterion, and high-order failure criterion.

In order to better reflect the basic properties and various situations of materials, Tsai-Wu failure criterion is selected to analyze the stress of the lining pipeline [20]. The general form of Tsai-Wu tensor polynomial failure criterion is:

$$F_i \sigma_i + F_{ij} \sigma_i \sigma_j + F_{ijk} \sigma_i \sigma_j \sigma_k = 1, \tag{10}$$

where *Fi*, *Fij* and *Fijk* represent the second-order tensor, the fourth-order tensor, the sixth-order tensor or higher order tensor, respectively (i, j, k = 1, 2, 3, … …, 6).

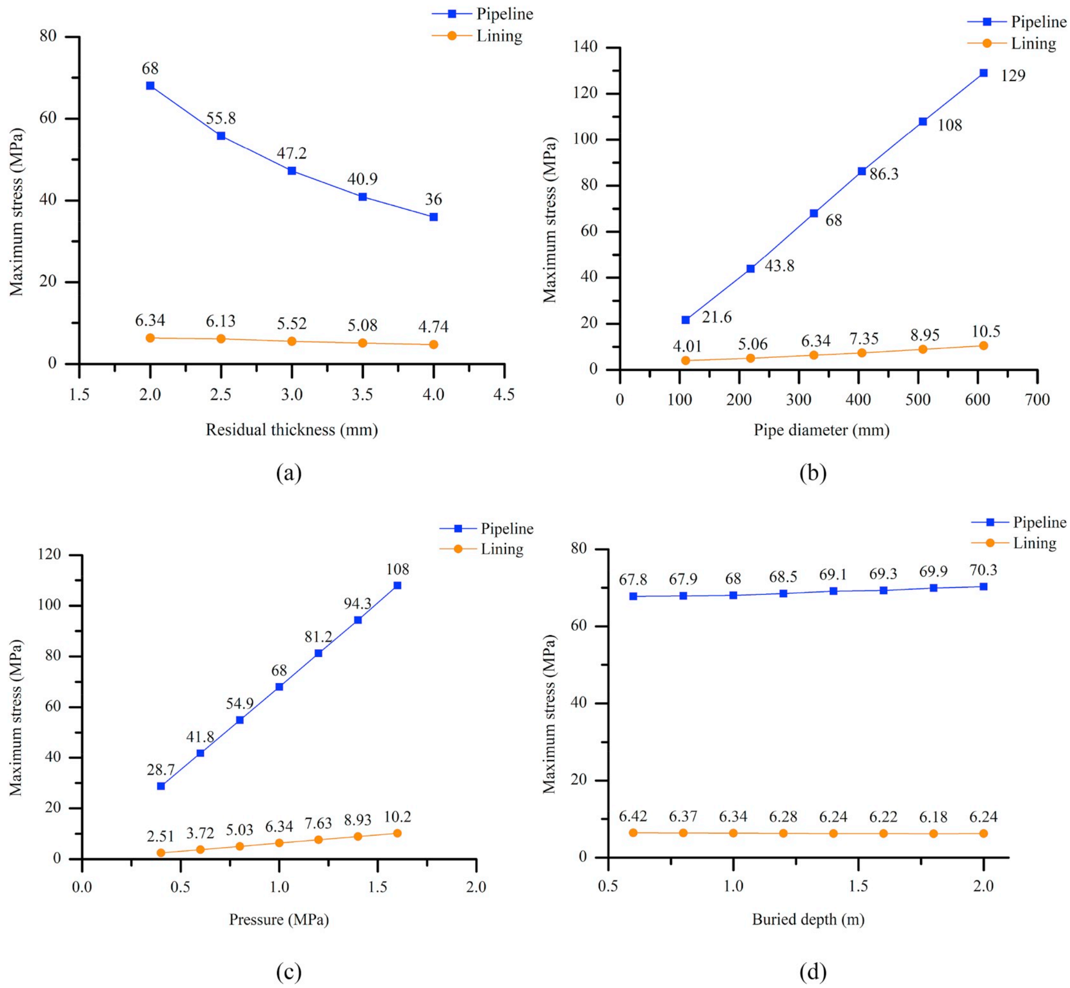

Fig. 14. The maximum stress of steel pipe and lining pipe with different influencing factors. (a) Residual thickness; (b) Diameter; (c) Pressure; (d) Buried depth.

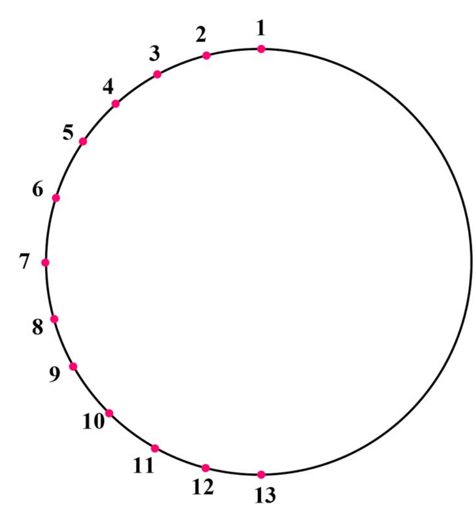

Fig. 15. Schematic diagram of perforation location.

4. Case study

This section describes the material properties that need to be used in FEA, the underlying assumptions of the material, and the settings in the numerical simulation.

4.1. Analysis object description

In this paper, the stress analysis of the pipe repaired by the IHL method under two corrosion conditions is carried out. The first one is under uniform corrosion condition, The original dimension of the steel pipe is 325 mm × 4.8 mm (diameter × wall thickness), and the uniform corrosion reduces the wall thickness to 2 mm, so the size of the steel pipe under uniform corrosion condition is 325 mm × 2 mm (diameter × wall thickness). The residual wall thickness is set to 2 mm because “SY/T 0087.1–2006: Standard of steel pipeline and tank corrosion assessment-Steel pipeline external corrosion direct assessment” [21] stipulates that for pipelines with volumetric corrosion defects, when the minimum residual wall thickness is less than 2 mm, the pipelines need to be repaired or replaced immediately. Moreover, the inner pressure is 1 MPa, and the buried depth of the pipe is 1 m. The outer wall of the lining is firmly attached to the inner wall of the steel pipe, so the lining has a diameter of 321 mm.

The other corrosion condition is corrosion perforation. The steel pipe size is 325 mm × 4.8 mm (diameter × wall thickness), but there is an elliptical hole in the pipe, and the other conditions are the same as the uniform corrosion.

4.2. Lining material

The lining materials studied in this paper are provided by ASOE house manufacturing Inc. (China), as shown in Fig. 3. The lining material has a three-layer structure, the outer layer is modified polyethylene

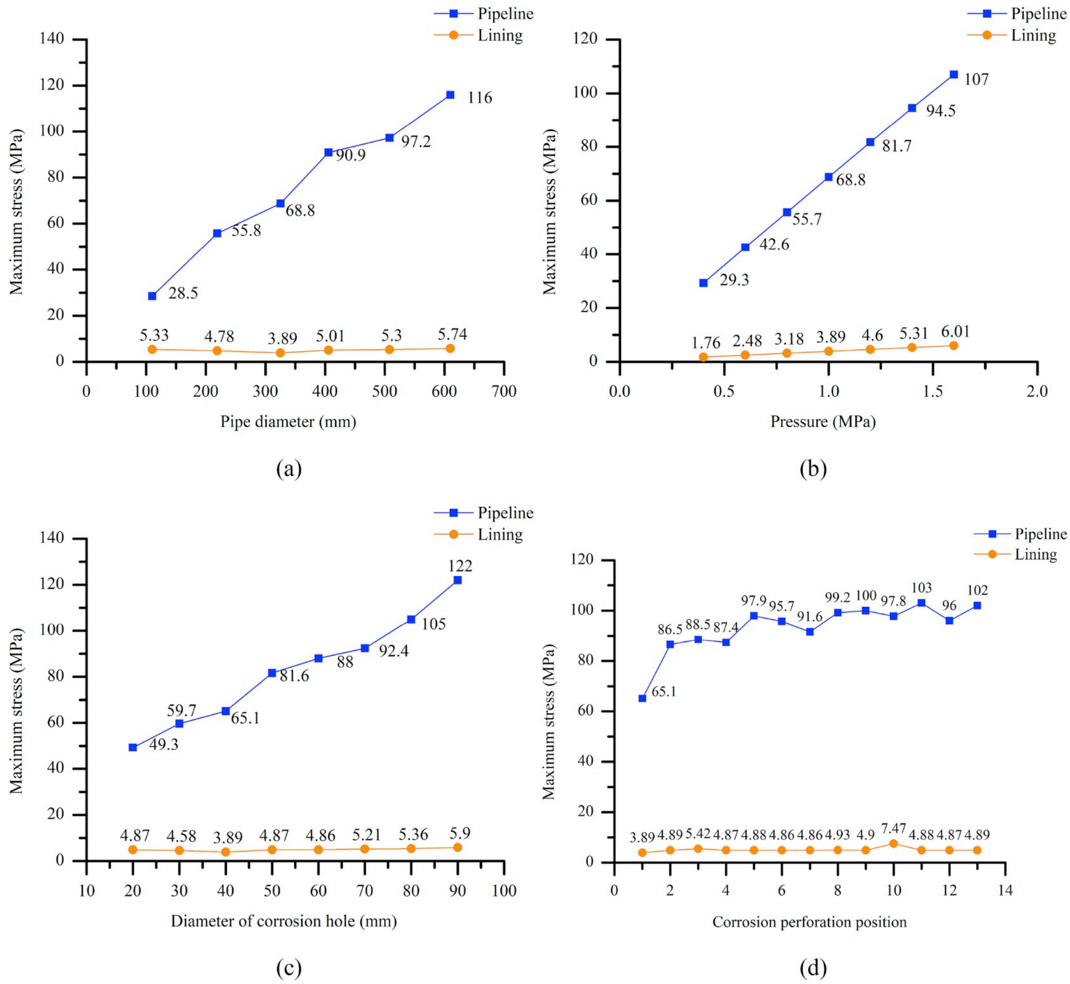

Fig. 16. The maximum stress of steel pipe and lining pipe with different influencing factors. (a) Diameter; (b) Pressure; (c) Diameter of corrosion hole; (d) Corrosion perforation position.

Table 6
Sensitivity analysis factors and base values.

Corrosion type	Factor	Base value
Uniform corrosion	Residual thickness	3 mm
	Pipe diameter	325 mm
	Pressure	1 MPa
	Buried depth	1.2 m
Corrosion perforation	Pipe diameter	325 mm
	Pressure	1 MPa
	Diameter of corrosion hole	50 mm

(PE), the middle layer is polyester filament, the inner layer is thermal polyurethane (TPU), as shown in Fig. 4, and their mechanical properties are shown in Table 2.

4.3. *Basic assumptions*

4.3.1. *Lining material*

The lining pipe is a composite material with a complex internal structure. To facilitate the analysis, the following underlying assumptions are made: (1) All components of the material are uniform and continuous, regardless of the possible material heterogeneity in actual production; (2) The interface between the layers of material is continuous; (3) The properties of matrix and fiber-reinforced layer in the composite are the same as before the composite, and the matrix and fiber-reinforced layer are isotropic; (4) There is no stress in the component material and composite before the load is applied. After applying the load, no transverse stress is generated between the matrix and the fiber-reinforced layer [19].

4.3.2. *Steel pipe*

The stress analysis of steel pipe needs some assumptions on the macro level: (1) The material structure of the steel pipe is continuous; (2) The material structure of the steel pipe is evenly distributed and isotropic; (3) Ignore changes in steel pipe geometry; (4) There is no original stress in the steel pipeline; (5) The flow parameters of the fluid in the pipe are considered to be time-independent.

4.4. *Numerical simulation*

4.4.1. *Geometric model*

The geometric model of FEA can be seen in Fig. 5. The buried depth of the pipeline is 1 m. Because the soil is an infinite space body, a specific range of soil as a research object needs to be selected. According to the Saint Venant's principle, soil length, width, and height are taken as 4 m. Since the geometric model is symmetrical, in order to save resources in the calculation process, half of the model is intercepted, that is, the model size is 4 m × 2 m × 4 m (length × width × height), as shown in Fig. 6.

4.4.2. *Material properties*

In this work, three materials need to be considered in FEA, including steel pipe, lining material, and soil material. The material properties of

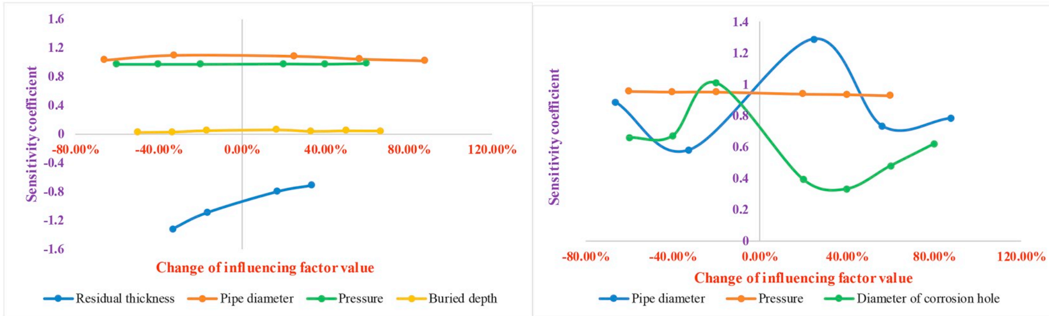

(a) (b)

Fig. 17. Sensitivity coefficient curve of steel pipeline stress. (a) Uniform corrosion conditions; (b) Corrosion perforation conditions.

Table 7
Applicable scope of steel pipe repaired by the IHL method under uniform corrosion conditions.

Pipeline size	Residual thickness (mm)	Allowable pressure (MPa)
DN200	2	2.9
	3	3.9
	4	5.2
DN300	2	1.9
	3	2.6
	4	3.5
DN400	2	1.5
	3	2.0
	4	2.6
DN500	2	1.1
	3	1.5
	4	2.0

Table 8
Applicable scope of steel pipe repaired by the IHL method under corrosion perforation conditions.

Pipe size	Corrosion hole diameter (mm)	Allowable pressure (MPa)
DN200	30	2.0
	40	2.2
	50	1.7
DN300	30	1.6
	40	1.8
	50	1.4
DN400	30	1.2
	40	1.4
	50	1.1
DN500	30	1.1
	40	1.2
	50	0.9

the steel pipe are shown in Table 3. The properties of the lining material are shown in Table 2, and the soil properties are shown in Table 4. The soil belongs to granular material. The compressive yield strength of this kind of material is far greater than the tensile yield strength, and when the material is subjected to shear force, the particle will expand, and its constitutive relationship is much more complicated than other materials, so Von Mises yield criterion is not suitable for this kind of material. In soil mechanics, the commonly used yield criteria are Drucker-Prager (DP) yield criterion and Mahr-Coulomb (MC) yield criterion. Some cases prove that the DP yield criterion is more suitable for the soil model. It can be expressed as [23]:

$$\sqrt{J_2} - \lambda I_1{}' + \kappa = 0 \tag{11}$$

where λ and κ represent material constants; J_2 represents the second invariant of the stress deviator tensor; $I_1{}'$ represents the first invariant of the stress tensor.

4.4.3. Mesh

In FEA, the establishment of the mesh can affect the accuracy of the calculation results to some extent. Because the research object is a pipeline, it is usually necessary to encrypt the mesh around the pipeline to improve the calculation accuracy. Under the condition of uniform corrosion, only the mesh around the pipe needs to be densified. Under the condition of corrosion perforation, as the corrosion hole is also the critical research object, it is also necessary to densify the mesh near the corrosion hole, as shown in Fig. 7.

4.4.4. Contact model

There are four contacts in the model established in this paper (see Fig. 8): (1) the type of face-to-face contact between the soil and the outer wall of the steel pipe is “no-separation”; (2) the type of face-to-face contact between the inner wall of the steel pipe and the outer layer of the lining (modified PE) is “no-separation”; (3) the type of face-to-face contact between the outer layer (modified PE) and the middle layer (polyester filament) of the lining is “bonded”; (4) the type of face-to-face contact between the middle layer (polyester filament) and the inner layer (TPU) of the lining is “bonded”.

4.4.5. Constraints and loads

The constraints and boundary conditions of the pipe-soil system are consistent under both corrosion conditions. Both the soil and the pipeline are subjected to vertical downward gravity, and the gravitational acceleration is 9.81 m/s^2. The inner wall of the lining is subjected to a pressure of 1 MPa. Four boundary conditions are set in the model: the lower surface of the soil is subject to fixed support (all displacement or rotation are limited), the three sides of the soil are subject to horizontal displacement constraints (downward movement is allowed), the upper surface of the soil is free constraints, and the symmetrical surfaces of the soil and the pipeline are set as symmetric constraints, as shown in Fig. 8.

5. Results

5.1. Uniform corrosion condition

Fig. 9 shows the stress analysis results of the steel pipe and the lining, the maximum stress of the steel pipe is 68 MPa, and the maximum stresses of the outer layer, the middle layer and the inner layer of the lining are 0.42 MPa, 6.34 MPa, and 0.321 MPa, respectively. It reveals that although the internal pressure is applied to the lining, the steel pipe is still the main pressure-bearing component, and the stress of the steel pipe is much larger than that of the lining. Moreover, the stress in the middle layer of the lining is much higher than the other two layers. Therefore, the middle layer is the leading pressure bearing component of the lining.

In order to study the repair effect of the lining, the stress of the steel pipe without the lining is also analyzed, as shown in Fig. 10. It reveals that if the pipeline is not repaired by the IHL method under uniform corrosion conditions, the maximum stress of the steel pipe is 77.4 MPa, indicating that the lining can effectively reduce the stress of the old pipeline. Fig. 11 can further illustrate that the stress of the steel pipe with the lining under different pressures is smaller than that of the steel pipe without the lining.

5.2. Corrosion perforation condition

In order to study the rehabilitation effect of the lining on the steel pipe with corrosion perforation, a corrosion perforation model is built, and the corrosion perforation position is located at the top of the pipe, as shown in Fig. 12. The shape of the corrosion hole is a regular ellipse, and the long axis of the ellipse is in the axial direction of the pipe. In this case, the corrosion hole has a long axis length of 40 mm and a short axis length of 20 mm.

Besides, in some cases, the corrosion hole can be considered as a circle. Therefore, this paper considers two corrosion perforation models: elliptical hole and circular hole. According to FEA results (see Fig. 13), the stress distribution characteristics of the two corrosion perforation models are similar, and the maximum stress appears in the axial position of the corrosion hole. In addition, the maximum stress of steel pipe in the elliptical hole model and circular hole model is 68.8 MPa and 65.1 MPa, respectively. It can be concluded that the risk of the elliptical corrosion hole condition is higher than that of the circular corrosion hole condition. For two cases of corrosion perforation, the maximum equivalent stress does not exceed its allowable stress 130 MPa, so the steel pipeline after the IHL rehabilitation can meet the safety requirement. Furthermore, the maximum stress of the pipeline without lining repair is 95.9 MPa in the elliptical corrosion hole condition, which shows that IHL repair can effectively solve the problem of corrosion perforation of the old pipeline.

6. Discussions

In order to make the conclusion more universal, it is necessary to explore the influencing factors. The influence of residual thickness, diameter, pressure, and buried depth on the stress of steel pipe with uniform corrosion is discussed. For the steel pipe with corrosion perforation, the influence of the location and size of corrosion perforation, the diameter and pressure of the pipe on the pipe stress is discussed. Table 5 lists the influencing factors and their value ranges.

6.1. Uniform corrosion

Fig. 14 shows the influence of various factors on the stress of steel pipe and lining under uniform corrosion conditions. The following conclusions can be drawn:

(1) As the remaining wall thickness decreases, the maximum stress of the steel pipe increases significantly, and the maximum stress of the lining increases slightly. With the increase in pipe diameter and transport pressure, the maximum stress of steel pipe and lining increases, and the stress rise trend of steel pipe is more prominent.
(2) As the buried depth of the pipeline increases, the maximum stress of the steel pipe does not change significantly, but it shows a small upward trend. There is no significant change in the maximum stress of the lining. It reveals that the influence of buried depth on pipeline stress is negligible.

6.2. Corrosion perforation

Under the condition of corrosion perforation, in order to facilitate the analysis, the circular hole is taken as the research object in the influence analysis of the corrosion hole size. The circular hole is also taken as the analysis object in the influence analysis of the corrosion hole position. From the pipe top to the bottom, thirteen locations are considered (see Fig. 15).

Fig. 16 shows the influence of several factors on the stress of steel pipe and lining under the corrosion perforation condition. From these analysis results, the following conclusions can be drawn:

(1) The stress of the steel pipe increases with the increase of the pipe diameter, but the stress of the lining has no noticeable change. Generally speaking, the stress of the lining decreases at first and then increases. The stress of the lining is the smallest when the pipe size is DN300.
(2) The maximum stress of steel pipe and lining increases with the increase of pressure, and the relationship between the maximum stress and pressure is basically linear. Moreover, the increasing trend of steel pipe stress is more evident than that of the lining.
(3) With the increase of corrosion hole diameter, the maximum stress of steel pipe also increases. However, the maximum stress of the lining does not change obviously, and the analysis shows that the maximum stress of the lining does not change monotonously with the corrosion hole diameter change.
(4) When the corrosion hole is located at the top of the pipe, the stress of the steel pipe is smaller than in other locations. When the location of the corrosion hole is close to the bottom of the pipe, the stress of the steel pipe is larger. Moreover, the maximum stress of the lining is less affected by the corrosion hole position, and the stress change trend of the lining is not consistent with the steel pipe.

6.3. Stress sensitivity analysis

In order to obtain the degree of influence of different factors on pipeline stress, this paper analyzes the sensitivity of pipeline stress under two corrosion conditions. The calculation equation of the sensitivity coefficient can be expressed as follows:

$$S=\frac{(\sigma_b-\sigma_t)\times F_b}{\sigma_b\times(F_b-F_t)} \tag{12}$$

where S represents the sensitivity coefficient. If S is greater than 0, the stress is positively correlated with the influencing factor; if S is less than 0, the stress is negatively correlated with the influencing factor. The larger the absolute value of S, the higher the influence of the factor on the stress; σ_b represents the base value of pipe stress; σ_t represents pipeline stress; F_b represents the base value of the influencing factor; F_t represents the value of influencing factor.

The sensitivity analysis factor usually needs to be a quantitative value, so the location of the corrosion hole is not considered in the sensitivity analysis, as shown in Table 6. The sensitivity analysis results are shown in Fig. 17. It can be concluded that under uniform corrosion conditions, the stress of the steel pipe is sensitive to changes in pipe diameter, pressure, and residual thickness, and is not sensitive to the buried depth. With the reduction of the residual thickness, the sensitivity of the pipe stress increases obviously. Therefore, in pipeline engineering, with the increase of service life and corrosion, the residual thickness should be regularly detected and repaired in time. In the case of corrosion perforation, the pipe stress is sensitive to the change of pipe diameter, pressure, and corrosion hole diameter, but they have different sensitivity change rules. The influence of pressure on the pipe stress is relatively constant, and the stress sensitivity of pipe diameter and corrosion hole diameter shows a trend of fluctuation.

6.4. Applicable scope of IHL technique

In engineering, in order to improve the design efficiency, it is necessary to provide a table to the engineers. Engineers can use the data in the table to identify the maximum pressure of an urban gas pipeline with uniform corrosion or identify the maximum corrosion size of the pipeline, as shown in Table 7 and Table 8.

7. Conclusions

In this paper, the finite element method is used to analyze the stress of two kinds of pipes with corrosion defects repaired by the IHL method, and the influencing factors are analyzed. The main conclusions are as follows:

(1) IHL method can effectively reduce the stress of the old pipeline, and the old pipeline is the primary pressure bearing component because its stress is much larger than the lining.
(2) The stress in the middle layer of the lining is much higher than that in the other two layers.
(3) Under the condition of uniform corrosion, the residual thickness is inversely related to the steel pipe stress, the pressure and diameter are positively related to the pipe stress, and the buried depth has little effect on the stress.
(4) Under the corrosion perforation condition, the pipe diameter, corrosion hole diameter, and pressure are positively correlated to the steel pipe stress. When the corrosion hole is at the top of the pipe, the pipe stress is minimal, and if the corrosion hole is near the bottom of the pipe, the stress is the largest.

Stress sensitivity is also analyzed in this paper. It is concluded that under uniform corrosion conditions, the pipe stress sensitivity is significantly improved with the decrease of residual thickness. However, under the condition of corrosion perforation, the influence of pipe diameter and corrosion hole diameter on pipe stress shows a fluctuation trend. Finally, this paper also gives the applicable scope of the IHL method, which can provide engineers with design information quickly.

Declaration of competing interest

The authors declare that they have no known competing financial interests or personal relationships that could have appeared to influence the work reported in this paper.

Acknowledgement

This article is funded by China Scholarship Council (201708030006).

References

[1] Lu H, Guo L, Azimi M, Huang K. Oil and Gas 4.0 era: a systematic review and outlook. Comput Ind 2019;111:68–90.
[2] Lu H, Behbahani S, Azimi M, Matthews J, Han S, Iseley T. A review of trenchless construction technologies for oil and gas pipelines. J Constr Eng Manag 2020. https://doi.org/10.1061/(ASCE)CO.1943-7862.0001819.
[3] Lu H, Ma X, Huang K, Azimi M. Carbon trading volume and price forecasting in China using multiple machine learning models. J Clean Prod 2020:119386. https://doi.org/10.1016/j.jclepro.2019.119386.
[4] Qiao W, Lu H, Zhou G, Azimi M, Yang Q, Tian W. A hybrid algorithm for carbon dioxide emissions forecasting based on improved lion swarm optimizer. J Clean Prod 2020:118612.
[5] Najafi M. Trenchless technology piping: installation and inspection: installation and inspection. McGraw Hill Professional; 2010.
[6] Matthews JC, Selvakumar A, Condit W. Current and emerging water main renewal technologies. J Infrastruct Syst 2012;19(2):231–41.
[7] Wood, E. (1977). U.S. Patent No. 4,009,063. Washington, DC: U.S. Patent and Trademark Office.
[8] Ma B, Najafi M. Development and applications of trenchless technology in China. Tunn Undergr Space Technol 2008;23(4):476–80.
[9] Wang YF, Yang ZG. Finite element analysis of residual thermal stress in ceramic-lined composite pipe prepared by centrifugal-SHS. Mater Sci Eng A 2007;460: 130–4.
[10] Li Z, Wang L, Guo Z, Shu H. Elastic buckling of cylindrical pipe linings with variable thickness encased in rigid host pipes. Thin-Walled Struct 2012;51:10–9.
[11] Rueda F, Otegui JL, Frontini P. Numerical tool to model collapse of polymeric liners in pipelines. Eng Fail Anal 2012;20:25–34.
[12] Chuk C, Urgessa G, Thippeswamy H. Numerical analysis of stresses for cured-in-place-pipe linings. WIT Trans Built Environ 2011;115:283–93.
[13] Kim YT, Haghpanah B, Ghosh R, Ali H, Hamouda AMS, Vaziri A. Instability of a cracked cylindrical shell reinforced by an elastic liner. Thin-Walled Struct 2013;70: 39–48.
[14] Shou KJ, Chen BC. Numerical analysis of the mechanical behaviors of pressurized underground pipelines rehabilitated by cured-in-place-pipe method. Tunn Undergr Space Technol 2018;71:544–54.
[15] Asoe. Unpublished water pipe rehabilitation design guide V3.0, pipe-in liner product. Taizhou, China: Asoe Manufacturing Inc.; 2018.
[16] Asoe. Unpublished water pipe rehabilitation installation guide V1.0, pipe-in liner product. Taizhou, China: Asoe Manufacturing Inc.; 2018.
[17] Berthelot JM, Ling FF. Composite materials: mechanical behavior and structural analysis. New York: Springer; 1999. p. 3–14.
[18] Kushnevsky V, Bledzki AK. The effect of interphase on residual thermal stresses. 2. Unidirectional fiber composite materials. Mech Compos Mater 1997;33(2):142–52.
[19] Niu Y. Stress analysis of gas pipeline repaired by liner pipe. Master thesis. Chengdu, China: Southwest Petroleum University; 2016.
[20] Narayanaswami R, Adelman HM. Evaluation of the tensor polynomial and Hoffman strength theories for composite materials. J Compos Mater 1977;11(4):366–77.
[21] CPPEI. SY/T 0087.1 Standard of steel pipeline and tank corrosion assessment-Steel pipeline external corrosion direct assessment. Beijing, China: Petroleum Industry Press; 2006.
[22] Yan X. Experimental and numerical evaluation of a new composite pressure pipe for a trenchless rehabilitation technology. Doctoral dissertation. Louisiana Tech University; 2016.
[23] Alejano LR, Bobet A. Drucker–prager criterion. In: The ISRM suggested methods for rock characterization, testing and monitoring. Cham: Springer; 2012. p. 247–52. 2007-2014.